Multiresolution modeling of large-scale ocean circulation

S. Danilov, Q. Wang, D. Sidorenko, R. Timmermann, C. Wekerle, V. Haid, X. Wang

Alfred Wegener Institute for Polar and Marine Research
Bremerhaven, Germany

1 Introduction

Large-scale ocean modeling today is almost exclusively based on models formulated on regular, structured meshes. These models have reached a high level of sophistication and offer users a wide selection of transport algorithms and parameterizations, together with practical experience accumulated over model histories. Many questions related to climate dynamics can be explored with their help either in a standing-alone mode or being coupled to a model of the atmosphere.

There are, however, certain arguments in favor of models capable to work on unstructured meshes. First, and most obviously, the strength of ocean currents is not uniform. Most intense currents are encountered in the equatorial belt, along western boundaries, between subtropical and subpolar gyres, and in the Southern Ocean. Besides, depending on the question to be explored, one may be interested in resolving eddy dynamics in a particular domain. If applied in this sense, unstructured meshes provide a tool for seamless nesting, which does not require solving the 'logistic' tasks associated with traditional nesting. Second, the internal Rossby radius in the ocean varies substantially with latitude, and unstructured meshes may help to create a setup with the resolution varying in proportion to the Rossby radius, i. e., 'uniformly' eddy permitting or resolving. Third, the dynamics of the ocean is in many places controlled by local features. For instance, the role of overflows in Gibraltar and Denmark Strait is well known. Similarly important are the processes of dense water formation over the periphery of the Southern Ocean or the presence of narrow straits (the Canadian Arctic Archipelago and Bering Strait to mention just few) which are frequently artificially modified in coarse climate models to allow for the exchange that would otherwise be blocked. On more global scales, resolving the continental shelf break may be of interest too, as in many places in the ocean there are currents confined to the vicinity of continental margins (i. e., in the Arctic Ocean or the Labrador Sea).

Bottom representation is one more area where unstructured meshes can be helpful. Surface meshes can be constructed so that they follow bathymetry, thus making the representation of bathymetry smoother even on meshes with geopotential vertical levels, see Fig. 1. On terrain following meshes, the ability to locally increase resolution over the steepest part of topography can be beneficial in minimizing the pressure gradient errors.

It is therefore believed that models capable of working on unstructured meshes may be convenient and optimal to use in certain tasks of ocean modeling. This does not imply that they will be able to fully replace models formulated on structured meshes — for one thing, those models are generally more CPU efficient, and for another, they also allow for some degree of mesh refinement. The most well-known examples are the meshes based on the Mercator projection and general orthogonal meshes which offer an increased resolution over a certain area. However, very frequently more freedom with mesh refinement is desirable, and unstructured-mesh models may be a better choice. It is also believed that with advancement of technology and optimizations the difference in computational efficiency between structured- and unstructured-mesh models will decrease.

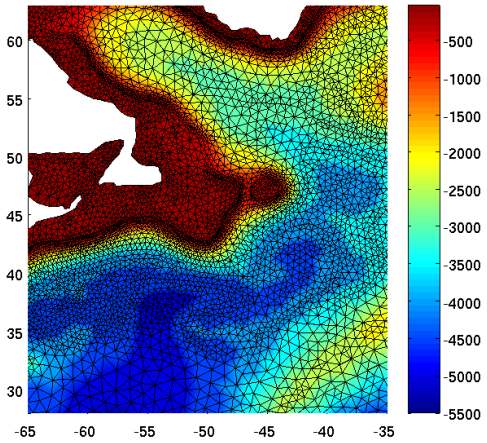

Figure 1: An example of triangular mesh. Such meshes can easily be constructed so that they follow bathymetry, with finer resolution over the continental shelf break. Color corresponds to the ocean depth in meters, axes are the longitude and latitude.

For the reasons mentioned above the interest towards unstructured meshes in large-scale ocean modeling is growing. FESOM is the first ocean general circulation model with such functionality (Danilov et al. (2004), Wang et al. (2008), Timmermann et al. (2009)). Other models are appearing now, including MPAS (Ringler et al. (2013)) and ICON (see the ICON web site). These groups use different numerical approaches, and we will learn in the next section about their advantages and disadvantages. Section 3 will discuss the examples of applications, followed by the Conclusions.

As an aside we note that the utility of unstructured meshes is much more obviously seen in coastal ocean modeling. In this case purely geometrical complexity of coastlines provides a decisive argument. Below we will discuss large-scale ocean modeling, but will mention coastal models too for illustration.

2 The main discretization types

There are two main types of approaches used to derive discretized equations on unstructured meshes — finite element (FE) and finite volume (FV) methods. Within the FE class one usually distinguishes between continuous Galerkin (CG) and discontinuous Galerkin (DG) discretizations. There are also approaches combining the elements of both. The FE approach assumes that unknown fields are expanded in a series of appropriate basis functions, and discretizes the equations by projecting them on a set of test functions. When the test functions coincide with the basis functions, one obtains the so-called Galerkin discretization. In the FV approach, the governing equations are integrated over control volumes, and divergences of flux terms are expressed via sums of outgoing fluxes. Basic principles of these methods are the subject of numerous books, and are briefly discussed in Danilov (2013).

In principle, unstructured meshes may be composed of various polygons. Most popular are triangular tessellations, but quads and hexagons present other options. The popularity of triangular meshes owes to their flexibility in varying resolution or fitting the mesh to the details of domain geometry. The degree of their flexibility can be learned from examples of coastal simulations that can be found at web sites of coastal models (ADCIRC or FVCOM). Large-scale models generally use less fancy meshes, but the freedom to vary the resolution in narrow passages is also needed (see, e.g., examples in Wekerle et al. (2013) or Scholz et al. (2013)). Quadrilateral unstructured meshes are less popular, as they

require strongly deformed elements in places where the resolution varies. In contrast, quasi-hexagonal Voronoi centroidal meshes are currently becoming popular and are used by the MPAS project (Ringler et al. (2013)). They are obtained by iterating the Voronoi tessellation until the cell generating points are sufficiently close to centroids, as explained by Ringler et al. (2013). If mesh resolution is varied smoothly most of the elements obtained in this iteration will be hexagons. We therefore present a brief description of popular discretizations that are used on triangular and quasi-hexagonal meshes. Since our goal here is only to make the reader acquainted with the status of research dealing with modeling on unstructured meshes, our description is by no way complete. We note that meshes used in ocean modeling are vertically aligned, so that the term 'unstructured' is related to the horizontal directions only. For this reason we will only discuss the horizontal discretizations.

2.1 FE triangular discretizations

The first unstructured-mesh ocean models had coastal focus and used the FE method (see the review by Pain et al. (2005) for a list of references). Some of them have been based on the so called $P_1 - P_1$ CG discretization. In this notation, P_1 stands for a polynomial of the first order (linear), and the first in the list is the discretization for the velocity field followed by the discretization for scalar quantities. If this discretization is used, the horizontal velocities (vector field) and the scalar fields (pressure, elevation, temperature and salinity) are all located at vertices of the triangular mesh. Any two-dimensional field $T(x,y,t)$ in this case is represented as $T = \sum T_i(t)N_i(x,y)$ where N_i is the linear test function equal to one at vertex i and going to zero at the nearest vertices. It is easy to see that the representation for T is just the linear interpolation between the vertices. This type of discretization is used by coastal models QUODDY and ADCIRC and the large-scale models FESOM (see e. g., Lynch et al. (1996), Westerink et al. (1992), Wang et al. (2008)).

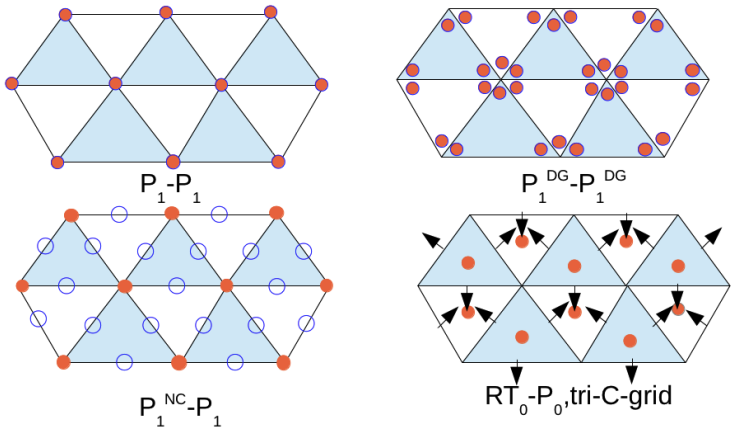

Figure 2: Most common triangular discretizations. Filled red circles correspond to scalar degrees of freedom, and blue circles to velocity degrees of freedom. $RT_0 - P_0$ operates with normal components of velocities shown by arrows.

The $P_1 - P_1$ discretization has certain deficiencies we will learn about soon, so other variants have been proposed. One of them is the $P_1^{NC} - P_1$ discretization, in this case the degrees of freedom of horizontal velocity are located on the edges, and scalar fields remain at vertices (see Figure 2). The superscript 'NC' stands for 'nonconforming'. The respective N_i in this case is equal to one at edge i, and -1 at the vertex opposing edge i. The field representation, albeit linear, is only continuous at edge midpoints.The

SLIM project (see White et al. (2008)) and the FESOM group (Danilov et al. (2008)) have been considering this scheme, and there are shallow-water codes based on this discretization. Although the P_1^{NC} velocity field has three times more degrees of freedom than the $P_1 - P_1$ representation, the $P_1^{NC} - P_1$ discretization does not demonstrate obvious advantages compared to $P_1 - P_1$.

One more possibility is still to use P_1 basis functions, but keep them restricted to individual triangles, which leads to discontinuous elements. In this case each of the triangles meeting at a vertex i has its own T_i, i. e., if, as is typically the case, six triangles meet at vertex i, there are six T_i restricted to their respective triangles (see Fig.2). Discontinuous linear elements ($P_1^{DG} - P_1^{DG}$) have been used by SLIM (Kärnä et al. (2012)) and have also been explored in some other coastal models. ICOM-Fluidity uses higher order discretization $P_1^{DG} - P_2$, which is well suited for representing the geostrophic balance (see, for example, Cotter and Ham (2011)). The topic of DG FE is discussed very often, as high-order DG FE schemes can simultaneously ensure high-order convergence and locality which may be beneficial for massive parallel implementations to come (see, for example, the presentation by F. Giraldo in this volume). On triangular meshes, however, low-order implementations (like P_1^{DG}) cluster their degrees of freedom without providing extra resolution compared to their continuous counterparts, and turn out to be computationally less efficient.

On regular quadrilateral meshes one of the traditional discretization choices is the Arakawa C-grid. Its FE implementation on triangular meshes is the so-called lowest-order Raviart-Thomas element (Raviart and Thomas , 1977), RT_0, and the discretization used is $RT_0 - P_0$. In this case the horizontal velocity field is expanded as $\mathbf{u} = \sum u_i \mathbf{N}_i$, where $\mathbf{N}_i = (\mathbf{r} - \mathbf{r}_i)/h_i$. Here, $\mathbf{r}$ and $\mathbf{r}_i$ are the radius vectors drawn to a point within a triangle and to vertex i of this triangle, respectively, and h_i is the height drawn from vertex i to the edge opposing it. It is easy to see that in this representation the u_i have the sense of normal velocities, and that the representation is continuous across the mesh edges for normal velocities but discontinuous for the tangent ones. More popular in ocean modeling is the FV analog of $RT_0 - P_0$, the triangular C-grid, and we postpone the discussion for a while.

Many other FE pairs have been proposed in the literature. While they are discussed theoretically, it is difficult to judge about their performance in realistic situations. We mention that a more detailed review can be found in Danilov (2013), and that Cotter and Shipton (2012) and Cotter and Thuburn (2012) present a procedure to construct new pairs with desirable properties.

2.2 FV triangular discretizations

FV discretizations on triangular meshes are less numerous. One can use the collocated variable placement, which will result in either vertex–vertex or cell-cell discretization, as illustrated in Fig. 3. In the first case, with each vertex we associate a median-dual control volume. Such a volume for vertex i is formed by connecting centroids of neighboring triangles with mid-points of edges emanating from i. Note that if the mesh is composed of equilateral triangles such control volumes are hexagons. Note also that vertex-vertex discretization is very similar to $P_1 - P_1$ in the FE case. Control volumes of the cell-cell discretization are the mesh triangles, and variables are stored at their baricenters. It would correspond to $P_0 - P_0$ in the FE case. One can also use a staggered cell-vertex discretization, which corresponds to $P_0 - P_1$ in the FE case. As concerns practical examples, vertex-vertex FVs have been discussed by Szmelter and Smolarkiewicz (2010) and Danilov (2012), and cell-vertex is used by FVCOM (Chen et al. (2003)) in coastal applications and was discussed in the large-scale context by Danilov (2012). These discretizations use full horizontal velocities. Triangular C-grids can also be easily implemented. They are widely used in coastal applications, with examples given by UnTRIM (Casulli and Walters (2000)) or SUNTANS (Fringer et al. (2006)), and also form the basis of ICON. They locate scalar fields at triangle circumcenters, with the implication that the circumcenters have to be located inside the triangles. Triangular meshes satisfying such properties are called orthogonal, and are less easy to generate (for example, all angles have to be acute). Their FE analog, $RT_0 - P_0$, does not have this limitation, but

on the expense of mass matrices appearing with the velocity time derivative.

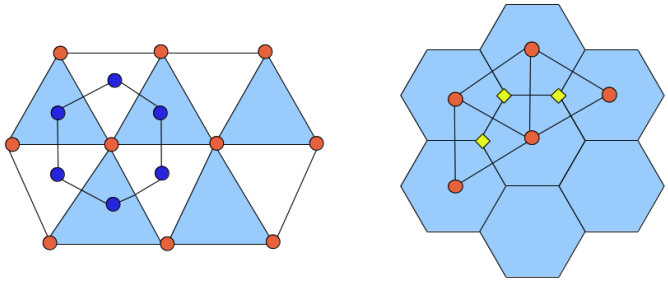

Figure 3: FV discretizations on triangular (left) and hexagonal (right) meshes. The filled red and blue circles correspond to, respectively, vertex and cell degrees of freedom on triangular meshes. Median-dual control volumes around vertices are hexagonal on meshes composed of equilateral triangles, so that vertex-vertex and cell-vertex discretization on triangles correspond to cell-cell and ZM discretizations on hexagons, respectively. In the case of ZM, velocities are at vertices (yellow rhombi). For C-grids, the number of scalar degrees of freedom on triangles is twice as large as on hexagons, while the number of velocity degrees of freedom is the same.

2.3 FV discretizations on quasi-hexagonal meshes

By connecting centers of quasi-hexagonal elements on Voronoi meshes one obtains a dual triangular mesh, and by connecting circumcenters of triangles on an orthogonal triangular mesh one will obtain quasi-hexagons. Such meshes are dual to each other, so in principle, except for details of control volumes, vertex-vertex triangular FV discretizations are similar to cell-cell quasi-hexagonal mesh discretizations. The cell-vertex triangular discretization is analogous to the ZM discretization proposed by Ringler and Randall (2002). The median-dual control volumes on triangular meshes deviate from hexagons in a general case, but the advantage is that the triangular mesh need not be orthogonal. They do coincide if triangles are equilateral.

Despite their seeming similarity the C-grid implementation on quasi-hexagonal meshes has rather different properties as compared to its triangular mesh counterpart. This stems from an approximately two times smaller number of scalar degrees of freedom available on a Voronoi mesh. As the result, a tri-C-grid and a hex-C-grid have very different balance between scalar and velocity degrees of freedom. Atmospheric example of a hexagonal cell-cell model is provided by the GME (Majewski et al. (2002)), and a hexagonal C-grid is the basis of MPAS (Ringler et al. (2013)).

2.4 A short discussion of discretizations

Why have so many different discretizations been proposed? The answer is that neither is perfect. First, for the simple staggered discretizations discussed here, there is a disbalance between the vector (velocity) and scalar degrees of freedom. It is well known that to properly represent dynamics one needs twice as many velocity degrees of freedom as used for scalar fields. All staggered discretizations mentioned above have either too many ($P_1^{NC} - P_1$, cell-vertex, hex-C-grid) or too little (tri-C-grid) velocity degrees of freedom, which leads to the presence of branches of spurious modes. One can learn about these modes

by taking linearized shallow water equations and performing the standard von Neumann analysis. And indeed, the discretizations with full velocity vectors ($P_1^{NC} - P_1$ and cell-vertex) prove to support spurious branches of inertial modes, i. e., oscillations at the Coriolis frequency with zero horizontal divergence, the hex-C-grid supports a spurious Rossby wave mode, and the tri-C-grid mixes spurious and physical gravity wave modes, which leads to a checkerboad pattern in the horizontal divergence field.

Second, simple collocated discretizations are balanced, but generally suffer from pressure modes. Here there are no spurious branches, but the behavior of physical branches deviates from the expected behavior, allowing for the presence of non-propagating perturbations. They owe their existence to a non-trivial null space of the discrete gradient operator. Many details pertaining to dispersive properties and modes of various discretizations can be found in the recent work by Le Roux (2012), which also contains references to previous studies. The issue of pressure modes is nicely discussed in the lecture by C. Cotter in this volume, which also explains how to construct balanced mixed (staggered) discretizations that are free of pressure modes.

While the subject is still under debate, the situation with practically 'tested' discretizations is that one can use them provided their spurious modes can be controlled without damaging the dynamics. This is the case with hex-C-grid and cell-vertex discretizations, where the available dissipative operators in the momentum equation are generally sufficient to maintain stability. It is less straightforward with discretizations where the spurious modes affect the scalar fields. Techniques to suppress the pressure modes are well known and long used, the challenge here is in proposing solutions compatible with volume and tracer conservation, which can be achieved, for example, following the FESOM algorithm (see Wang et al. (2008) and Danilov (2012)). Such techniques may, however, lead to some energy imbalance. Spurious divergence noise of a triangular C-grid can be strongly suppressed through divergence averaging, yet a more consistent technology requires a modification of the velocity field (as proposed by P. Korn).

Although the linear analysis is very enlightening, one needs to study the performance of the full discretized primitive equations in eddy regimes to make final conclusions. Such regimes are characterized by cascades of enstrophy and scalar variance to small scales. A discretization should be able to maintain stable performance in this case without excessively strong dissipation. A non-trivial aspect here is the difference in the resolution of scalar and vector degrees of freedom for staggered discretizations, which may require special measures.

The lesson learned from the development of FESOM, which is the first large-scale unstructured-mesh model with a practical record, is that the CG FE discretization presents a suboptimal choice for large-scale ocean models. For one thing, it couples time derivatives through mass-matrices $M_{ij} = \int N_i N_j d\Omega$, where the integration is over the domain, which entails the overhead of their inversion. For another, it introduces horizontal connections even in vertical differentiation operators. Dealing with both either slows down the performance or introduces additional compromises (for more detail see Danilov (2013)). Since the DG FE codes turn out to be slow at present, the FV method seems to offer the most suitable platform for future development. Not surprisingly, MPAS, ICON and the FESOM follow-up, targeting at CPU-efficient unstructured-mesh codes, are all using the FV method.

We now turn to applications run with FESOM. While the appearing new unstructured-mesh models will surpass it in CPU efficiency, it is sufficiently efficient for many practical tasks which illustrate the utility of unstructured meshes.

3 FESOM and applications performed with it

FESOM is a primitive equation ocean model working on unstructured triangular meshes, coupled to an unstructured-mesh sea ice model. Numerics of FESOM is described by Wang et al. (2008) and

Timmermann et al. (2009), and the recent status of the code is described by Wang et al. (2013). FESOM has been coupled to the ECHAM6 atmospheric model (Stevens et al. (2013)), which enables one to use it for climate studies (Sidorenko et al., (2013)). Except for the fact that it uses unstructured triangular meshes and CG FE discretization, it behaves in many respects as other ocean circulation models intended for climate or long-term ocean-only applications, but it offers the opportunity to refine the mesh where necessary. FESOM participated (albeit a bit late) in the CORE1 intercomparison project (Sidorenko et al. (2011)) addressing the long-term behavior and trends of various models used for climate relevant studies, and shows similar performance. Now it takes part in the COREII intercomparison with focus on the interannual variability of the ocean circulation. The mean climate state of the ECHAM6-FESOM coupled system shows trend and variability that compare very favorably against models of the CMIP5 class (Sidorenko et al., (2013)).

As has already been mentioned, the FESOM discretization is based on linear functions. The nodes of the 3D mesh are vertically aligned with the surface mesh. They are located on level surfaces which can be geopotential, terrain following or a combination of both. The surface triangular mesh and the set of interior levels define prismatic elements. In the current implementation each prism is split further into tetrahedra. This has the advantage that the 3D basis functions remain linear independent from the inclination of level surfaces, and all 3D fields are then given by 3D linear interpolation $T(x,y,z,t) = \sum T_i(t)N_i(x,y,z)$. On prismatic meshes the prisms are deformed if level surfaces deviate from geopotential surfaces and numerical integration is performed approximately, with lower efficiency, using quadrature points.

We continue with examples of applications run with FESOM.

3.1 Freshwater transport through the Canadian Arctic Archipelago

The freshwater exchange of the Arctic Ocean with the North Atlantic happens partly trough Fram Strait and partly through the straits of the Canadian Arctic Archipelago (CAA). The excessive freshwater storage in the Arctic is due to precipitation and runoff of numerous rivers, and the outflow is largely driven by the pressure difference between the Arctic and the North Atlantic. Since the path of freshwater lies in the vicinity of main convection sites, the redistribution of freshwater between Fram Strait and the CAA has global implications, in particular on the strength of the meridional overturning circulation (MOC).

The transport of freshwater through the CAA is mostly associated with volume transport. Most of the current climate models simulate it by artificially increasing the width of major channels (Parry Channel and Nares Strait). While this may be sufficient to simulate the mean transport, it is not necessarily so for the transport variability. The study by Wekerle et al. (2013) explores these issues by comparing the performance of two global model versions, the control configuration with 24 km resolution in the CAA, which is common for climate models, and the other one with 5 km resolution in the CAA. Both resolve the Arctic Ocean with 24 km, getting coarser in the rest of the ocean except for the vicinity of coastlines. The fine resolution of the CAA (see Fig. 4) adds about 50% nodes to the surface mesh and limits the time step to be about 10 min, yet the model is still fast enough to allow for multidecadal simulations.

The comparison between the simulation results and available observational data by Wekerle et al. (2013) demonstrates that the fine resolution run is indeed able to simulate the transport variability in closer agreement with the observational data. Further analysis shows that the freshwater transported through the CAA stays confined to the coast in the Labrador Current, while the increased salinity in the Eastern and Western Greenland Currents in the fine-resolution run leads to an increased mixed layer depth in the Labrador Sea, which, in turn, increases the strength of the MOC. The analysis also shows that the variability in freshwater transport is driven by the large-scale atmospheric pressure system. The global impact of the regional improvement indicates the potential of unstructured meshes in climate

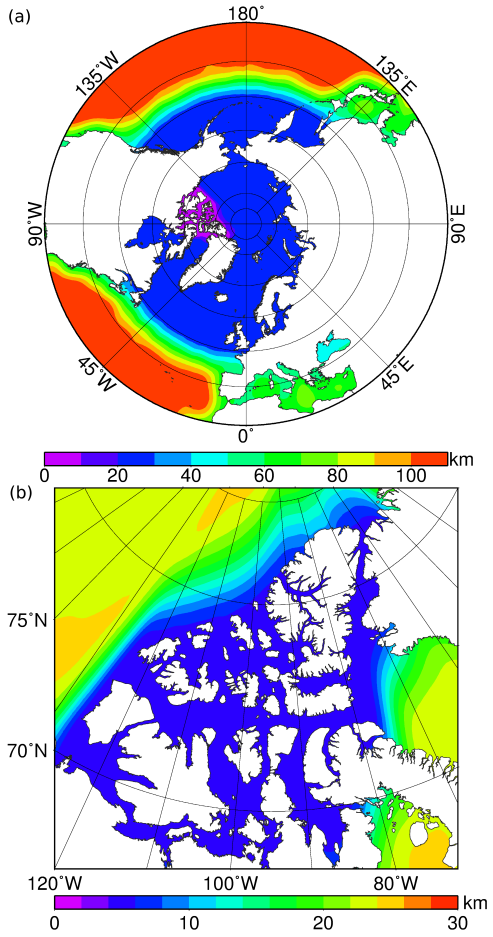

Figure 4: Horizontal resolution of the mesh with the CAA region refined used by Wekerle et al (2013): (a) view in the stereographic projection and (b) zoomed into the CAA region.

simulations.

3.2 Outflows in the Ross and Weddell Seas

Wang et al. (2009, 2010); Wang et al. (2012) apply FESOM to learn about the dynamics of overflows and Antarctic Bottom Water (AABW) in the Weddell and Ross Seas. In these cases FESOM is used in regional configurations with open boundaries, but its ability of local refinement is still crucial, as the resolution is varied from about one degree to several km or even less (to 0.5 km in Wang et al. (2010)) in the area of overflows. The domain of integration should be sufficiently large to ensure that the influence of open boundaries is negligible, and fine resolution in the overflow region is needed to properly simulate the dynamics and accompanying mixing and entrainment. The local radius of deformation based on the plume height and density contrast has a scale of several kilometers so that eddy dynamics can be modeled only if sufficiently small scales are resolved. The goal of such studies is to obtain estimates of deep water formation rates and to learn about the mechanisms causing their variability. The regional configuration is used here either to minimize computational effort or to include tides, and in each case the focus is on the local processes. The study of Wang et al. (2009) explores the role of topographic ridges in shaping the overflow in the Southern Weddell Sea demonstrating that they influence the descent of dense water and its mixing with surrounding waters. There are areas where tides may modify the AABW formation. In particular, this is the case for the other major overflow in the Southern Ocean – the north-western

Ross Sea overflow. The study by Wang et al. (2010) explores it in detail showing that the presence of tides increases the AABW production and modifies the pathway and properties of newly formed AABW through mixing and advection (see Fig. 5). The study by Wang et al. (2012) focuses on the variability of the Weddell Sea overflow showing that it is intervoven into the dynamics of the entire Weddell Gyre. The outflow at the shelf is in geostrophic balance and thus its transport is influenced by the density contrast between the outflow and intruding ambient water. The properties of ambient water depend on the variability of wind forcing, as the strength of wind curl determines the depth of isopycnals at the coast. All these studies reveal interesting dynamics and FESOM with its ability to locally resolve small scales is a convenient tool in this context.

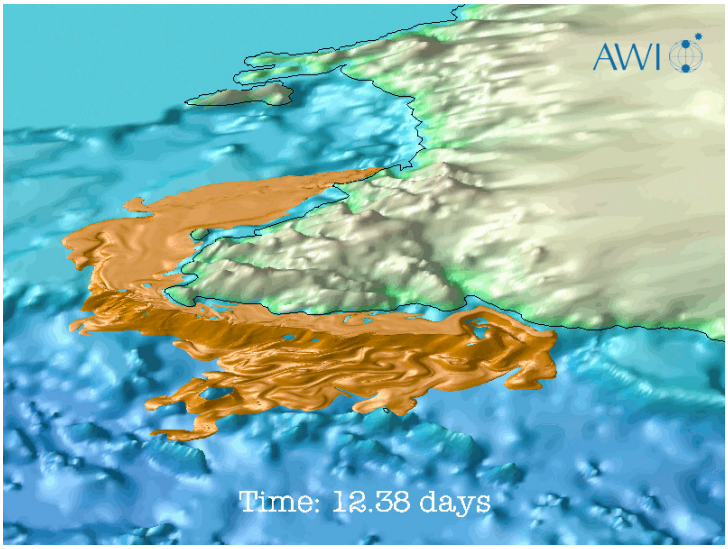

Figure 5: Simulated AABW formation from the northwestern Ross Sea. A passive tracer with concentration c=1 is injected to the source of dense water over the inner continental shelf. The isosurface of c=0.1 is shown, which indicates the plume of recently ventilated AABW. A movie can be found at http://www.awi.de/?id=6209.

3.3 Antarctic ice shelf basal melting

It their recent work Timmermann et al. (2012), Hellmer et al. (2012) and Timmermann and Hellmer (2013) studied basal melting of the Antarctic ice shelf. The assessment of the basal melting rate is of immense interest in the context of global warming, as the increased melting, apart from its impact on ocean watermasses, may lead to changes in the ice sheet grounding line location and to a reduction of ice sheet stability, with implications for an accelerating sea level rise. Since the geometry of ice cavities is rather complex, and some of them are of small size, simulations of melting dynamics require a model capable of resolving complex geometry of ice cavities, which in turn demands a mesh on a few kilometer scale, and terrain following vertical levels inside the cavity. FESOM provides this refinement in a global setup, and also allows to combine the terrain following vertical coordinate inside the cavity with the geopotential (z-) coordinate in the rest of ocean. The setup and its performance analysis against available observations are described by Timmermann et al. (2012). Hellmer et al. (2012) did twenty-first-century projections by using the atmospheric forcing derived from the HadCM3 atmospheric model output concluding "that a redirection of the coastal current into the Filchner Trough and underneath the Filchner-Ronne Ice Shelf during the second half of the twenty-first century would lead to increased movement of warm waters into the deep southern ice-shelf cavity", which leads to strongly increased basal melting in large parts of the ice shelf (Fig.6). Timmermann and Hellmer (2013) continued this

study and compared the effect of atmospheric forcing derived from two climate models, HadCM3 and ECHAM5/MPI-OM, noting that in the second case the trends are small and concluding that surface heat and salt fluxes over the continental shelves in the marginal seas of the Southern Ocean are crucial for the future of large cold water ice shelves in the Ross and Weddell Seas.

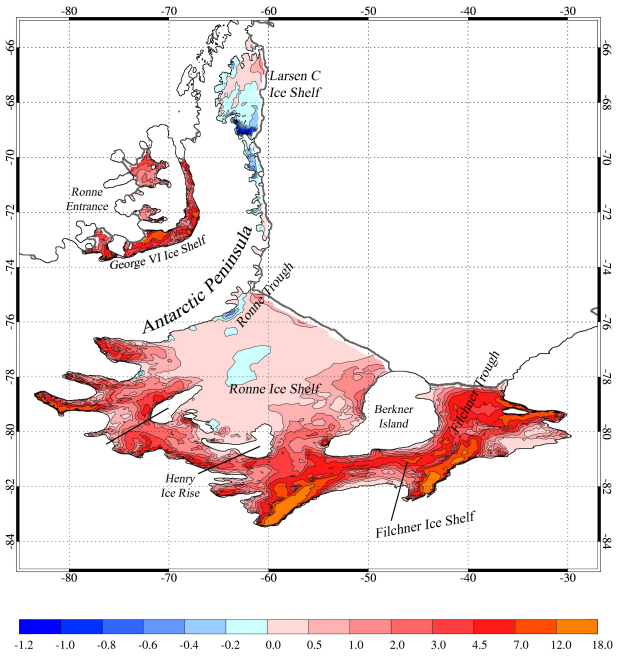

Figure 6: Increase of basal melt rates (m/yr) for Filchner-Ronne, Larsen C, and George VI Ice Shelves during the 22nd century in a simulation forced with HadCM3 data for the IPCC's A1B scenario (ten-year average 2140-2149 minus 1990-1999 mean). Note the non-linear color scale.

3.4 Other studies

There are other research topics where the choice of FESOM as a modeling tool has been natural and dictated by the dynamics to be studied. Haid and Timmermann (2013) explored the impact of coastal polynias in the southern Weddell Sea on the ice formation on a local scale and with respect to the whole basin. On the technical side, this task requires a resolution on the scale of a few kilometers close to the coast, over the shelf and the continental shelf break in a global configuration, which is provided by FESOM. Polynias occur in the presence of offshore winds which drive the ice off the coast and expose the ocean to cold air. Ocean cooling across the open water is much stronger than that over the area covered with ice, which leads to increased ice production, brine rejection and the descent of the newly formed salty water down to the bottom. The mean winter heat flux to the atmosphere (Figure 6a) features strong maxima in very narrow stretches along the coastline where recurrent polynyas form. The mean winter heat flux from the ocean (Figure 6b) shows prominent maxima associated with upwelling at the continental shelf break and distinct small-scale maxima in regions where polynyas occur. These patterns indicate that even in winter, when most of the water column is close to the freezing point, heat supplied by warmer water of deep ocean origin is a non-negligible component of the surface energy budget and modifies (in fact reduces) the rate of sea ice formation.

A question naturally arises about the impact of polynias on the ocean dynamics and sea ice volume

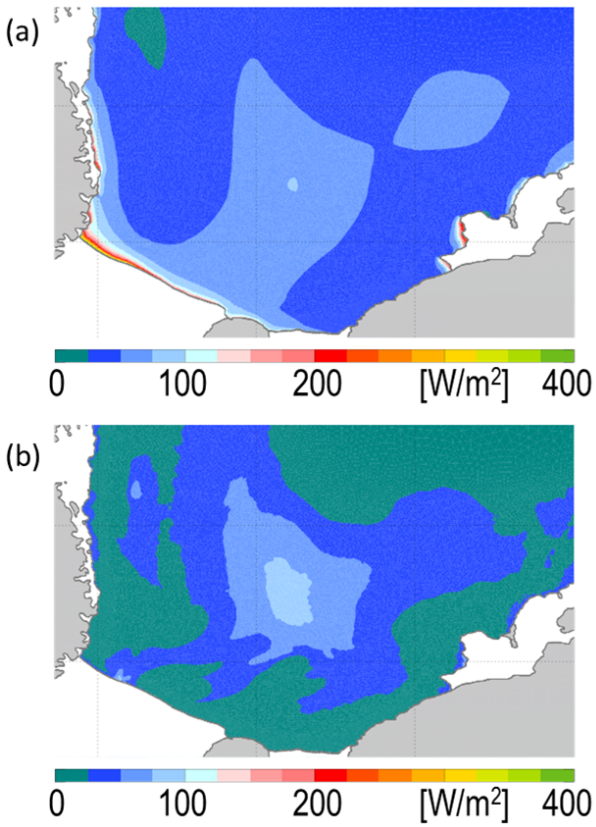

Figure 7: Mean heat flux (upward positive) in the southwestern Weddell Sea averaged over the months May-September 1990-2009 (a) at the lower boundary of the atmosphere and (b) at the upper boundary of the ocean.

formation. Should, for example, a climate model include the parameterized effect of polynias in a way that goes beyond the traditional representation as a signature of reduced ice thickness and concentration? Haid and Timmermann (2013) show that ice formation at polynias is indeed very intense, and in the Southern Weddell Sea contributes about 11% of total ice production although the area occupied by them is less than 0.6%. Its contribution to the total ice production in the Weddell Sea is less significant, so that the impact of polynias on the ice budget is certainly not negligible, but also not decisive.

Studies of Wang et al. (2012) and Scholz et al. (2013) exploit the potential of FESOM only partly, as they deal with meshes having only a moderate stretching factor. Nevertheless, the refinements they provide are essential for the studies performed. The first one focuses on the implications of increased Greenland Ice Sheet melting, and is performed on a global mesh of about 1.3 degree resolution refined to 25 km around Greenland. It analyses the changes in sea level height of steric origin and pathways of the released freshwater, showing that the dynamical sea level rise is expected in the northern North Atlantic and in the Arctic. Reliable estimates of the sea level rise would require the estimates of increased melting rate, which is uncertain. However the pathways of added freshwater are determined by dynamics and should not significantly depend on the melt water release rate. The second study focuses on the comparison of interannual to decadal variability simulated with FESOM with the available observational data. Its mesh is refined to 7-20 km in the Labrador Sea, 10-20 km near the Greenland Scotland Ridge and to 35-75 km in the central Weddell Sea and in the Ross Sea, with minimum values that are in the order of 10 km. Further refinements are made in the equatorial belt and along coastlines. The intention here was to get an improved representation in the regions involved in deep water production and has

indeed led to a setup which compares favorably with observations. One of conclusions derived from this comparison is that the model setup performs very well in areas with high resolution.

4 Conclusions

Large-scale ocean modeling on unstructured meshes is gradually becoming reality. Clearly, models formulated on regular meshes will dominate in the modeling community in the near future because of their computational efficiency. Yet unstructured meshes have a lot to offer, and depending on the practical task, they can be more convenient to use and more efficient. Most of the practical large-scale unstructured-mesh applications available thus far have been performed with FESOM. The examples shown here indicate the potential of unstructured-mesh methods.

FESOM is based on the $P_1 - P_1$ FE discretization. Due to the need to handle large matrices, it is less efficient numerically than the appearing FV codes such as MPAS (Ringler et al. (2013)), ICON, or the cell-vertex code being developed at the AWI (Danilov (2012)). Although these models are still slower per degree of freedom than the regular mesh codes, the difference is rather moderate, and is more than acceptable given the new possibilities (see the comparison of MPAS and POP performance in Ringler et al. (2013)). All discretizations in models used now or being developed suffer from spurious modes, but in many cases there are solutions for handling them, and the preference to a particular discretization depends on whether the modes can be suppressed with minimum consequences. There is ongoing work on new balanced discretizations, and it remains to see whether they will lead to practical advantages.

Many issues have been left outside this lecture. Development of parameterizations suited for variable meshes and high-accuracy advection schemes are among key research topics remaining in the community. The mutual influence of fine- and coarse-resolved dynamics presents an open question too. Increasing experience in practical applications and the appearance of new setups are advancing the unstructured-mesh technology, and we hope that climate research will benefit from it in the future.

References

Casulli V, Walters RA (2000) An unstructured grid, three-dimensional model based on the shallow water equations. Int J Numer Meth Fluids 32: 331–348

Chen, C., Liu, H., Beardsley, R. C., 2003. An unstructured grid, finite-volume, three-dimensional, primitive equations ocean model: Applications to coastal ocean and estuaries. J. Atmos. Ocean. Tech. 20, 159–186.

Cotter, C. J., Ham, D. A., 2011. Numerical wave propagation for the triangular $P1_{DG} - P2$ finite element pair. J. Comput. Phys. 230, 2806–2820.

Cotter, C. J., Shipton, J., 2012. Mixed finite elements for numerical weather prediction. J. Comput. Phys. 231, 7076-7091.

Cotter, C. J., Thuburn, J. 2012. A finite element exterior calculus framework for the rotating shallow-water equations. arXiv:1207.3336v01.

Danilov S, Kivman G, Schröter J (2004) A finite element ocean model: principles and evaluation. Ocean Modelling 6, 125–150.

Danilov. S., Wang, Q., Losch, M., Sidorenko, D., Schröter, J., 2008. Modeling ocean circulation on unstructured meshes: comparison of two horizontal discretizations. Ocean Dynamics 58, 365–374.

Danilov, S., 2010. On utility of triangular C-grid type discretization for numerical modeling of large-scale ocean flows, Ocean Dynamics 60(6), 1361-1369.

Danilov, S., 2012. Two finite-volume unstructured mesh models for large-scale ocean modeling. Ocean Modell. 47, 14–25, doi:10.1016/j.ocemod.2012.01.004.

Danilov, S., 2013. Ocean modeling on unstructured meshes. Ocean Modell. 69, 195–210

Fringer, O. B., Gerritsen, M., Street, R. L., 2006. An unstructured-grid, finite-volume, nonhydrostatic, parallel coastal ocean simulator. Ocean Modelling 14, 139–173.

Haid, V. and Timmermann, R. (2013) Simulated heat flux and sea ice production at coastal polynyas in the southwestern Weddell Sea, J. Geophys. Res., 118 , 2640–2652, doi:10.1002/jgrc.20133

Hellmer, H. H., Kauker, F., Timmermann, R., Determann, J. and Rae, J. (2012) Twenty-first-century warming of a large Antarctic ice-shelf cavity by a redirected coastal current , Nature, 485 (7397), pp. 225-228. doi:10.1038/nature11064

Kärnä, T., Legat, V., Deleersnijder. E. A baroclinic discontinuous Galerkin finite element model for coastal flows. Ocean Modelling, http://dx.doi.org/10.1016/j.ocemod.2012.09.009

Le Roux, D. Y., 2012. Spurious inertial oscillations in shallow-water models. J. Comput. Phys. 231, 7959–7987.

Lynch, D. R., Ip, J. T. C., Naimie, C. E., Werner, F. E. (1996) Comprehensive coastal circulation model with application to the Gulf of Maine. Cont. Shelf Res., 16, 875–906.

Majewski, D., Liermann, D., Prohl, P., Ritter, B., Buchhold, M., Hanisch, T., Paul, G., Wergen, W., Baumgardner, J. (2002) The Operational Global Icosahedral-Hexagonal Gridpoint Model GME: Description and High-Resolution Tests. Mon. Wea. Rev., 130, 319–338.

Pain, C. C., Piggott, M. D., Goddard, A. J. H., Fang, F., Gorman, G. J., Marshall, D. P., Eaton, M. D., Power, P. W., de Oliveira, C. R. E. (2005) Three-dimensional unstructured mesh ocean modelling, Ocean Modelling, 10, 5-33.

Raviart, P. A., Thomas J. M., 1977. A mixed finite element method for 2nd order elliptic problems. In Mathematical Aspects of the Finite Element Methods, Galligani I, Magenes E (eds). Lecture Notes in Mathematics. Springer: Berlin, 292–315.

Ringler, T. D., Randall, D. A., 2002. The ZM grid: an alternative to the Z grid. Mon. Wea. Rev. 130, 1411–1422.

Ringler, T., Petersen, M., Higdon, R., Jacobsen, D., Maltrud, M., Jones, P. W., 2013, A Multi-Resolution Approach to Global Ocean Modelling, 69, 211–232.

Scholz, P., Lohmann, G., Wang, Q., Danilov, S. (2013) Evaluation of a Finite-Element Sea-Ice Ocean Model (FESOM) set-up to study the interannual to decadal variability in the deep-water formation rates. Ocean Dynamics, 63, 347–370, doi:10.1007/s10236-012-0590-0

Sidorenko, D., Wang, Q., Danilov, S., Schröter, J., 2011. FESOM under Coordinated Ocean-ice Reference Experiment forcing. Ocean Dynamics 61, 881–810, doi:10.1007/s10236-011-0406-7.

Sidorenko D., Rackow, T., Jung, T., Semmler, T., Barbi, D., Danilov, D., Dorn, W., Dethloff, K., Goessling, H. F., Handorf, D., Harig, S., Hiller, W., Juricke, S., Schröter, J., Wang, Q., Fieg, K. (2013) Towards multi-resolution global climate modeling with ECHAM6-FESOM. Part I: Model formulation and mean climate. Clim. Dyn., submitted.

Stevens, B., Giorgetta, M., Esch, M., Mauritsen, T., Crueger, T., Rast, S., Salzmann, M., Schmidt, H., Bader, J., Block, K., Brokopf, R., Fast, I., Kinne, S., Kornblueh, L., Lohmann, U., Pincus, R., Reichler, T., Roeckner, E., 2013. Atmospheric component of the MPI-M Earth System Model: ECHAM6. J. Adv. Model. Earth Syst.

Szmelter, J., Smolarkiewicz, P., 2010. An edge-based unstructured mesh discretization in geospherical framework, J. Comput. Phys. 229, 4980-4995.

Timmermann, R., Danilov, S., Schröter, J., Böning, C., Sidorenko, D., Rollenhagen, K., 2009. Ocean circulation and sea ice distribution in a finite-element global ice–ocean model. Ocean Modelling 27, 114–129

Timmermann, R., Wang, Q. and Hellmer, H. (2012) Ice shelf basal melting in a global finite-element sea ice/ice shelf/ocean model, Annals of Glaciology, 53, doi:10.3189/2012AoG60A156

Timmermann, R. and Hellmer, H. (2013) Southern Ocean warming and increased ice shelf basal melting in the twenty-first and twenty-second centuries based on coupled ice-ocean finite-element modelling, Ocean Dynamics, doi:10.1007/s10236-013-0642-0

Wang, Q., Danilov, S., Schröter, J., 2008. Finite Element Ocean circulation Model based on triangular prismatic elements, with application in studying the effect of topography representation. J. Geophys. Res. 113, C05015. doi:10.1029/2007JC004482

Wang, Q., Danilov, S., Schröter, J., 2009. Bottom water formation in the southern Weddell Sea and the influence of submarine ridges: Idealized numerical simulations. Ocean Modelling 28: 50–59

Wang, Q., Danilov, S., Hellmer, H., Schröter, J., 2010. Overflow dynamics and bottom water formation in the western Ross Sea: The influence of tides, J. Geophys. Res. 115, C10054, doi:10.1029/2010JC006189.

Wang, X., Wang, Q., Sidorenko, D., Danilov, S. Schröter, J., Jung, T., 2012. Long-term ocean simulations in FESOM: evaluation and application in studying the impact of Greenland Ice Sheet melting. Ocean Dyn. DOI: 10.1007/s10236-012-0572-2.

Wang, Q., Danilov, S., Fahrbach, E., Schröter, J., Jung, T. (2012) On the impact of wind forcing on the seasonal variability of Weddell Sea Bottom Water transport. Geophys. Res. Lett., 39, L06603. doi:10.1029/2012GL051198.

Wang, Q., Danilov, S., Sidorenko, D., Timmermann, R., Wekerle, C., Wang, X., Jung, T., Schröter, J. (2013) The Finite Element Sea ice-Ocean Model (FESOM): Formulation of an ocean general circulation model. Submitted to Geosci. Model Dev.

Wekerle, C., Wang, Q., Danilov, S., Jung, T., Schröter, J. (2013) The Canadian Arctic Archipelago throughflow in a multiresolution global model: Model assessment and the driving mechanism of interannual variabilityJ. Geophys. Res., 118, 1–17, doi:10.1002/jgrc.20330

Westerink, J. J., Luettich, R. A., Blain, C. A., Scheffner, N. W., 1992. ADCIRC: An Advanced Three-Dimensional Circulation Model for Shelves, Coasts and Estuaries; Report 2: Users Manual for ADCIRC-2DDI. Contractors Report to the US Army Corps of Engineers. Washington D.C.

White, L., Deleersnijder, E., Legat, V., 2008a. A three-dimensional unstructured mesh shallow-water model, with application to the flows around an island and in a wind driven, elongated basin. Ocean Modell. 22, 26–47.